ISSN: 1410-8917
e-ISSN: 2597-9914

Jurnal Kimia Sains dan Aplikasi 25 (4) (2022): 137–145

Jurnal Kimia Sains dan Aplikasi
Journal of Scientific and Applied Chemistry

Journal homepage: http://ejournal.undip.ac.id/index.php/ksa

# Silica-rich Sodalite Synthesis: The Effect of Variations in Ultrasound Treatment and Hydrothermal Temperature

Sriatun [a,*], Martha Chandra Annike Putri [a], Hanifa Zakiyatul Urbach [a], Adi Darmawan [a], Widayat [b], Heru Susanto [b]

[a] Department of Chemistry, Faculty of Science and Mathematics, Diponegoro University, Semarang, Indonesia
[b] Department of Chemical Engineering, Faculty of Engineering, Diponegoro University, Semarang, Indonesia

*Corresponding author: sriatun@live.undip.ac.id

https://doi.org/10.14710/jksa.25.4.137-145

Article Info

Article history:

Received: 10th November 2021
Revised: 20th March 2022
Accepted: 23rd March 2022
Online: 30th April 2022

Keywords:
Silica-rich sodalite; ultrasound; hydrothermal; crystallinity; hydrophobicity

Abstract

Silica-rich sodalite zeolite has been synthesized by ultrasound treatment and hydrothermal temperature variation. This study aimed to determine the effect of ultrasound treatment and hydrothermal temperature variations on the crystallinity, hydrophobicity, and structural properties of silica-rich sodalite zeolite. The synthesis was conducted by reacting a sodium aluminate and sodium silicate solution by varying Si/Al ratios of 20, 30, 40, 60, 80, and 90. The next step was to characterize the product. The product with the best crystallinity was used as a reference to determine the effect of ultrasound and hydrothermal temperature. The reaction gel was treated with and without ultrasound and hydrothermal using autoclave at 100, 150, and 200°C for 24 hours. The last step was the product characterization using XRD, FTIR, and GSA. The XRD showed similarity peaks at 2θ = 14.058°; 24.41°; 31.73°; 34.75°; 42.88°. The best crystallinity was silica-rich sodalite zeolite with a Si/Al ratio of 30. Meanwhile, silica-rich sodalite zeolite peaks were obtained at 2θ = 14.16°, 24.66°, 31.99°, 35.13°, and 43.39° by ultrasound treatment and hydrothermal temperature variation (100, 150, and 200°C). Ultrasound treatment revealed the presence of other peaks besides sodalite at 2θ = 19.05° and 27°, where these peaks were referred to as SAPO-56. In conclusion, the degree of crystallinity increased with increasing temperature, decreasing Si-OH/Si-O-Si showed increased hydrophobic properties. Increasing the hydrothermal temperature of 150 and 200°C with and without ultrasound treatment increased the surface area significantly to 114.137 $m^2/g$ and 160.717 $m^2/g$, and the pore volume of sodalite with a Si/Al ratio of 30 to 0.318 cc/g and 0.274 cc/g.

## 1. Introduction

Sodalite is an essential host molecule for creating a simple periodic arrangement of various types of synthetic zeolites. Sodalite is not only a framework for zeolite A (LTA) but also a skeleton building unit for other zeolite types such as Hexagonal MFI (EMT), Faujasite (FAU), Franzinite (FRA), Giuseppettite (GIU), Linde Type N (LTN), Marinellite (MAR), and Tschortnerite (TSC) [1]. The morphology of silica sodalite is cubic crystal, spherical aggregates, disoriented octahedral-faced cubes, and imperfect spherical threaded balls, depending on the experimental conditions [2]. The increase in Si concentration is responsible for the morphological changes of silica sodalite in which octahedral and dodecahedral modifications are dominant. In addition, the increasing Si concentration causes the silica sodalite size to become less uniform. High-silica sodalites exhibit identical properties such as large surface area and pore volume (related to the skeleton's density) and hydrophobicity. Therefore, high-silica sodalites are widely used as adsorbents, heterogeneous base catalysts, and matrix membranes [3].

The Si/Al ratio significantly influences the framework composition, and this condition will affect the

phase change process from sol to gel. The amount of silica and alumina in the solution will affect the phase of crystal, crystallization rate, and the concentration of $OH^-$ ions [4]. The internal structure of the zeolite can be controlled by adjusting the Si/Al ratio, such as Si/Al with ratio of 1.1 and 1.3, which produced sodalite and analcime, and the ratio of 2 and 2.5 produced analcime [5].

High-alumina zeolite has several weaknesses. The synthesis using a low Si/Al ratio will affect the properties of the resulting zeolite, such as skeleton shape, pore volume, surface area, hydrophobicity, and low adsorption capacity [5]. Theoretically, a high Si/Al silica ratio shows identical properties such as surface area, large pore volume (related to the skeleton's density), and hydrophobicity (the higher hydrophobicity, the greater adsorption capacity) [6]. Therefore, high-silica zeolites are widely applied as adsorption, catalysts, and membranes [7].

Zeolite can be synthesized using various methods, including hydrothermal [8, 9, 10], alkaline desilication fusion [11, 12], ultrasound [13, 14, 15], microwave [16, 17, 18], and template addition [19, 20, 21]. This study used ultrasound and hydrothermal methods [22] for producing silica-rich sodalite zeolite. The hydrothermal method is relatively simple without using complicated and expensive equipment. Besides that, that method also has several advantages, such as a fast heating rate, a rapid reaction process, better yield, high purity, and high efficiency of energy transformation. The ultrasound-assisted porous material synthesis method is simple with a short synthesis time and does not require complicated facilities. When ultrasound energy acts on a liquid medium, the microbubbles in the liquid expand and then burst. The bursting of bubbles produces a mixing effect on a micro-scale, accelerating the dissolution and nucleation processes and crystal growth [23].

The hydrothermal method for preparing sodalite has been widely studied by several research papers. Kumar and Jena [24] synthesized hydroxy sodalite from fly ash using a hydrothermal process with a temperature of 150°C for 20 hours. Luo *et al.* [25] synthesized sodalite using fly ash from Mianyang at 100°C for 12 hours, and the zeolite product was used for lead adsorption. A similar study was conducted by Li *et al.* [26], using the temperature of 160°C for 24 hours, where the sodalite product was used for nitrogen adsorption. Sari *et al.* [9] synthesized sodalite with $Na_2O/Al_2O_3$ ratios of 10, 20, 30, and 40 at 100°C for 24 hours, and the best sodalite was produced at a ratio of 20.

Mu *et al.* [22] synthesized SSZ-13 zeolite using hydrothermal and ultrasound methods by varying time processes. The best products were obtained for 30 minutes and a temperature of 160°C. The result indicates that ultrasound shortens the crystal formation time and requires a low temperature. A similar study conducted by Behin *et al.* [27] successfully synthesized NaP zeolite from clinoptilolite by varying ultrasound time to produce NaP zeolite with uniform crystals. Dere Ozdemir and Piskin [28] reported that a crystallinity of 79.64% could be obtained by synthesizing zeolite A from fly ash using the ultrasound method for 2 hours at 110°C. That result indicates that the ultrasound method can improve crystallinity. Khoshbin and Karimzadeh [11] synthesized ZSM-5 by varying ultrasound times. The optimum conditions for obtaining ZSM-5 were at 190°C for 20 minutes.

According to the background explanation, one of the challenges in the zeolite synthesis process is the long crystallization time. The ultrasound-assisted was chosen as one of the pretreatment methods that can shorten the formation time of zeolites and other microporous and mesoporous materials [22]. This study aimed to produce the silica-rich sodalite zeolite using ultrasound pretreatment followed by hydrothermal crystallization at 100, 150, and 200°C. For comparison, samples treated with hydrothermal methods were also prepared.

## 2. Methodology

### 2.1. Materials and equipment

The materials used were sodium silicate ($Na_2SiO_3$ solution, Merck), aluminum hydroxide (powder ($Al(OH)_3$, Merck), sodium hydroxide (NaOH pellets, Merck), and distilled water. The equipment used in the synthesis and analysis were pH meter (Macherey-Nagel), analytical balance (Ohaus), autoclave, hotplate (JlabTech), oven (Shimadzu), Ultrasound (Pro+), XRD (Philip Analytical JOEL JDX-3530), FTIR Spectroscopy (PerkinElmer Spectrum Version 10.03.06), and GSA (Quantachrome NovaWin).

### 2.2. Experiment

#### 2.2.1. Determination of Si/Al ratio by hydrothermal method

As a preliminary step, silica-rich sodalite was synthesized by hydrothermal method with Si/Al ratios of 20, 30, 40, 60, 80, and 90. Mole ratio 0.14 NaOH: 0.0058 $Al(OH)_3$: x $Na_2SiO_3$: 1.15 $H_2O$ with x was varied according to the Si/Al ratio. NaOH was dissolved in hot distilled water, and then $Al(OH)_3$ was added until dissolved. The sodium aluminate solution was added to the sodium silicate solution dropwise. After forming the aluminosilicate gel, the hydrothermal process was continued in an autoclave at 200°C for 24 hours. The product was washed until a neutral pH, dried, and characterized by FTIR and XRD.

#### 2.2.2. Determination of the temperature and ultrasound treatment effects on silica-rich sodalite

The next step was the synthesis of silica-rich sodalite zeolite with a Si/Al ratio of 30 (the product with the best crystallinity from the previous step). After gel formation, the hydrothermal process was performed at 100, 150, and 200°C for 24 hours, respectively. After that, the synthesized solids were neutralized and dried. These products were coded as TS 100, TS 150, and TS 200. Meanwhile, ultrasound treatment was applied prior to the hydrothermal process at each temperature variation using ultrasound at a frequency of 40 kHz, 100 W for 30 minutes. Ultrasound treatment products were coded as US 100, US 150, and US 200. As a final step, all synthesis products were characterized by FTIR and XRD, and the best product was characterized by GSA.

## 3. Results and Discussion

The aluminate and silicate species reaction caused the solution to become viscous like a gel. The gel formation indicates a strong interaction due to the polymerization of silicate ions and aluminate ions. The formation of zeolite crystals occurs when condensation is accompanied by polymerization in a supersaturated solution. The solid phase is formed as an amorphous gel, and the solution phase as a supersaturated solution is in equilibrium. The amorphous gel will dissolve and undergo structural rearrangement to form species that are the seeds of the crystal nucleus and in the nucleation stage [29]. At that stage, the Si/Al ratio affects a change from sol to gel [30].

At this stage in the solution, there is an equilibrium between the remaining amorphous gel crystal core seeds and the supersaturated solution. If the remaining gel dissolves, crystal growth will occur until the gel is completely dissolved. The gel underwent a hydrothermal process in an autoclave at a variation temperature of 100, 150, and 200°C for 24 hours. The hydrothermal process aimed to homogenize the crystals formed and perfect the growth of zeolite crystals [4]. The hydrothermal process involves water and heat, where the mixture is heated to a high temperature in a tightly closed vessel. This situation is intended so that there is an equilibrium between water vapor and solution; thus, no water evaporates, and the composition of the solution remains. At this hydrothermal stage, a condensation reaction occurs, which allows the formation of new bonds such as Al-O-Si and Si-O-Si [31].

### 3.1. Silica-rich Sodalite Crystallinity

The XRD diffractograms of silica-rich sodalite with Si/Al ratios of 20, 30, 40, 60, 80, and 90 by the hydrothermal method are shown in Figure 1. The diffractogram with a clear peak separation pattern, high peak intensity, and sharpness of the peak indicates that the product has excellent crystallinity. The peaks that appeared at nearly the same 2θ diffraction angle indicate the same type of mineral as each other [32].

The silica-rich sodalite zeolite with a Si/Al ratio of 30 diffractograms showed a diffraction angle (2θ) 14.058°; 24.41°; 31.73°; 34.75°; 42.88°, which was similar to the standard RRUFF ID R040636 at 2θ 13.9°; 24.42°; 27.94°; 30.146°; 35.03°; 36.76°; 42.53°. The sodalite peaks in this study correspond to the sodalite obtained by the stirring aging treatment for 72 hours by Pourali and Samadi-Maybodi [33]. The peaks of synthesized sodalite were also in accordance with the sodalite obtained by transforming kaolin using 3 M NaOH and a hydrothermal time of 24 hours [8]. It can be concluded that the sample has a crystalline phase if its diffractogram has sharp and high-intensity peaks. This is agreed with the research by Vongvoradit and Worathanakul [34] that temperature and crystallization time affected the crystallinity of SUZ-4. The higher intensity showed the high crystallinity and the narrower FWHM (full width half maximum) at a 2θ angle.

According to this information, the order of crystallinity in Figure 1 was Si/Al ratio of 30 > 40 > 20, where the peaks corresponded to sodalite. Meanwhile, Si/Al ratios of 60, 80, and 90 were amorphous phases.

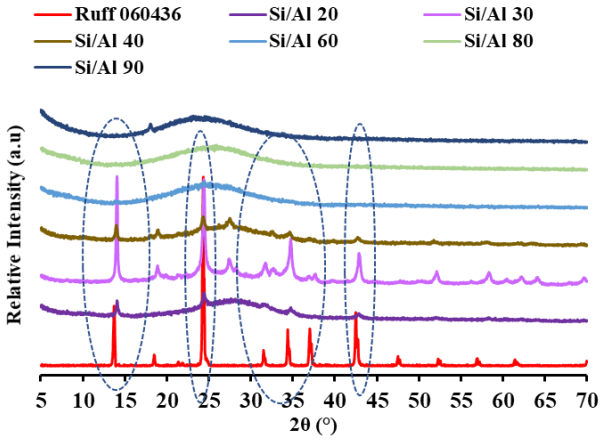


**Figure 1.** Diffractogram of the synthesized product with Si/Al ratio variation using the hydrothermal method and RUFF 060436

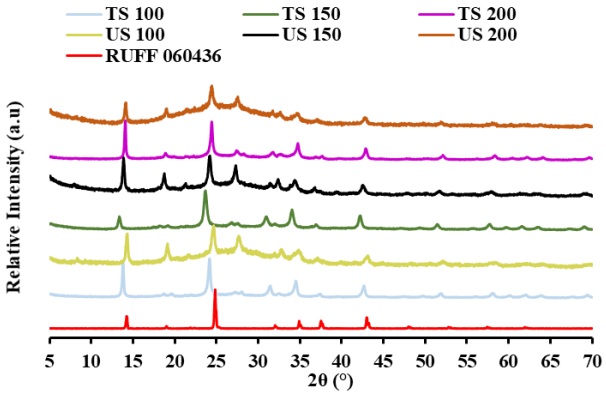


**Figure 2.** Diffractogram of silica-rich sodalite zeolite with and without ultrasound treatment and RUFF 060436

The diffractogram pattern in Figure 2 of all samples shows a similar 2θ diffraction angle. The diffraction angle (2θ) of samples was similar to RUFF 060436 standard sodalite at 2θ = 14.16°, 24.66°, 31.99°, 35.13°, and 43.39° successively according to the crystal plane (110), (211), (310), (222), and (330) [19]. Based on Figure 2, there are differences in peak sharpness of silica-rich sodalite zeolite without and with ultrasound treatment. Silica-rich sodalite without ultrasound had better crystallinity than ultrasound with increasing temperature. As a result of ultrasound treatment, silica-rich sodalite zeolite exhibited a lower crystallinity because the intensity of the diffraction peak appeared to decrease and become broader. Even at a temperature of 200°C, the crystallinity dropped drastically. However, the sodalite was evident by peaks at diffraction angles of 2θ = 19.05° and 27°. When combined with 2θ = 43.39°, it referred to the peak of SAPO-56. The decrease in crystallinity may be due to the energy given being too high, causing the crystal growth to be damaged. In the ultrasound treatment, peaks appeared at 2θ = 19.05° and 27°, whereas these peaks did not appear in the treatment without ultrasound, so it is possible that the higher the temperature will form stable crystals.

Stable crystals do not quickly change to a metastable phase that is easily soluble when washed. The zeolite crystal formation stage occurs during the heating (hydrothermal) process. Amorphous gels undergo rearrangement to form a different structural arrangement that is more regular, resulting in the formation of a crystal nucleus embryo. At the metastable state (easy to change), an equilibrium is reached between the crystalline nucleus embryo, the residual amorphous gel, and the supersaturated fluid. If the residual amorphous gel dissolves once more, there will be crystal growth of the nucleus embryo until the remaining amorphous gel is depleted and stable crystals are formed [35]. A mineral must be highly stable and have a low energy structure to persist for an extended period. A physical system's general stability condition corresponds to a minimum free energy G (of Gibbs) [36].

The mechanical effect of ultrasound treatment increases the dissolution of solid particles suspended in the liquid phase. This results in an amorphous aluminosilicate gel in the form of a precipitate. The slowing of nucleation in the intermediate aluminosilicate gel prevents the formation of zeolite crystals, although ultrasound treatment enhances dissolution. Late sonication (conventional heating followed by UST irradiation) successfully synthesized zeolite [37, 38].

Another research studied the synthesis of NaP zeolite using ultrasound at 150–290 W for 3–6 hours followed by hydrothermal at 100°C for 12 hours and 24 hours. The results showed that the formation of NaP zeolite occurred by applying 150 W ultrasound for 3 hours. In addition, the increasing energy and time only showed a slight effect on the formation of zeolite. Moreover, the crystallinity of the powder decreased gradually with increasing irradiation time. Ultrasound-induced shock waves and cavitation into the reaction medium stabilizes the particles at a smaller size to prevent the growth of particles into large crystalline solids. In addition, the fast heating/cooling rate during bubble evolution leads to the reduction of the crystallinity of nanoparticles to the formation of an amorphous structure. In conclusion, increasing the temperature resulted in lower crystallinity of the synthesized zeolite [39]. The decrease in crystallinity due to ultrasound treatment also occurred in the synthesis of Na-A by Vaičiukynienė *et al.* [13].

### 3.2. Functional Group of Silica-rich Sodalite

The characterization using Fourier transform infrared (FTIR) was intended to determine the functional group of the synthesized sodalite zeolite. The FTIR analysis was conducted at 400–4000 $cm^{-1}$. Meanwhile, the specific peak of the sodalite zeolite was in the range of the wavenumber 400–1300 $cm^{-1}$. The FTIR spectra pattern of the synthetic product at various Si/Al ratios of 20, 30, 40, 60, 80, and 90 is shown in Figure 3.

Figure 3 shows that all samples have absorption bands at ~585 $cm^{-1}$, indicating single four-rings of sodalite building blocks. Wavenumber ~1037 $cm^{-1}$ indicates the presence of Si-O-T stretching vibrations. Based on these findings, there is a typical absorption of sodalite zeolite, although the absorption is not as strong as it should be due to the early stages of nucleation. This also indicates that the zeolite synthesized at each Si/Al ratio is sodalite zeolite, but the crystallinity has not entirely formed yet. The absorption at a wavenumber of ~450 $cm^{-1}$ that appears in each product is a bending vibration of the T-O-T bond, where T is Si or Al atom [4]. According to Shukla and Pandya [40], an absorption band at 550 $cm^{-1}$ near 450 $cm^{-1}$ indicates sodalite formation.

Product with Si/Al ratios of 30, 60, 80, and 90 had adsorption bands on wavenumbers of 793 $cm^{-1}$, 793 $cm^{-1}$, 796 $cm^{-1}$, and 797 $cm^{-1}$, respectively. The absorption indicates the T-O-T bond symmetry stretching vibration. Meanwhile, the T-O-T bond symmetric stretching vibration absorption band appears at 713 $cm^{-1}$ for the ratios of 20 and 40. Absorption in the area of 1600–1650 $cm^{-1}$ is H-O-H bending vibration. In addition, there is also stretching of the -OH group in silanol (Si-OH) at ~3700 $cm^{-1}$ [25].

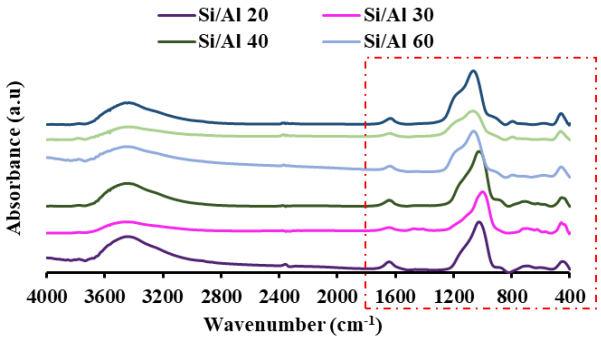


**Figure 3.** FTIR spectra of the synthesized product with Si/Al ratio variation using the hydrothermal method

The FTIR spectra of silica-rich sodalite with a Si/Al ratio of 30 prepared under ultrasound and hydrothermal treatment by varying hydrothermal temperatures of 100, 150, and 200°C are presented in Figure 4. Figure 4 shows that the spectra of all synthesized products are similar. The difference lies in several peaks that appear at certain absorptions. Besides that, the difference in the absorption intensity of the peaks also indicates a difference in zeolite formation. The sharper the absorption intensity, the more structures or functional groups formed.

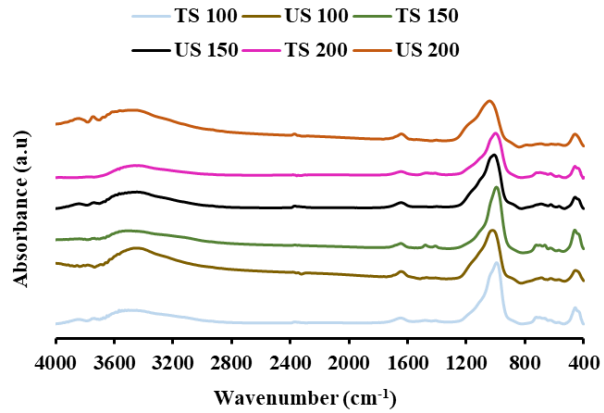


**Figure 4.** FTIR spectra of silica-rich sodalite zeolite with and without ultrasound treatment

The absorption band of silica-rich sodalite zeolite at all hydrothermal temperatures and ultrasound treatment

shows a specific area of sodalite at 500–650 $cm^{-1}$, which is single four-rings (S4R) sodalite. The absorption band at 1630–1640 $cm^{-1}$ corresponds to the O-H group of water molecules absorbed by the zeolite. The strain vibration of the –OH group is shown at 3100–3800 $cm^{-1}$. In the sodalite framework, the –OH group causes hydrogen bonds to silica at 3400 $cm^{-1}$ [41].

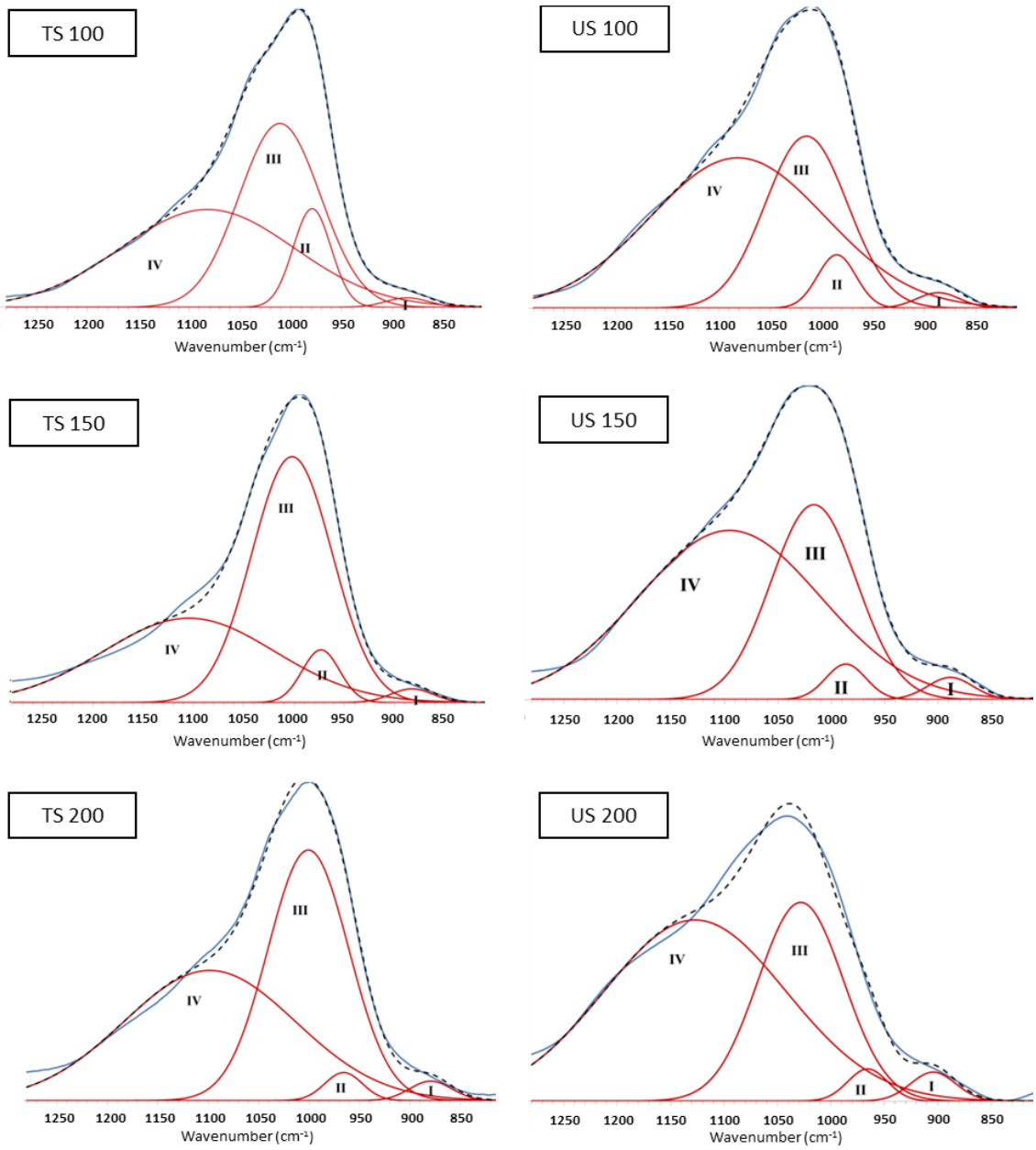


**Figure 5.** Deconvolution of silica-rich sodalite zeolite with and without ultrasound treatment

The spectra of all silica-rich sodalites with a Si/Al ratio of 30 prepared under both treatments showed similarities. Therefore, a quantitative analysis was investigated by comparing the derivative curves of the FTIR spectra on the mainframe of sodalite. The derivative curve was obtained using Fityk software with Gaussian calculations to find the derivative curve. The derivative curves for the six spectra are presented in Figure 5.

Furthermore, the area of Si-OH deconvolution (deconvolution peak II) is compared to the area of Si-O-T (deconvolution peak III), the ratio of Si-OH/Si-O-Si is obtained. The ratio of Si-OH/Si-O-Si is presented in Figure 6. Figure 6 shows that the Si-OH/Si-O-Si ratio decreases with and without ultrasound treatment when the hydrothermal temperature increases. The trend indicates that the Si-OH group will continue to react and form a Si-O-Si framework when the increasing temperature. Increasing the hydrothermal temperature without ultrasound treatment will accelerate crystal formation. Temperature provides energy to enhance crystallization; thus, a higher temperature causes Si-OH to decrease while the number of Si-O-Si increases. This is in line with Potapov and Zhuravlev [42] on the dependence of silanol Si-OH concentration at a temperature of 200–1200°C. Likewise, when employing ultrasound treatment, ultrasound waves can control the nucleation process to increase the rate of crystal formation. When ultrasound energy plays a role in a liquid

medium, the microbubbles contained in the liquid will enlarge and then burst. The bursting of bubbles will accelerate the process of nucleation and crystal growth. Therefore, it can be understood that the ratio of Si-OH/Si-O-Si with ultrasound treatment is always higher than without ultrasound treatment at each of the same temperatures.

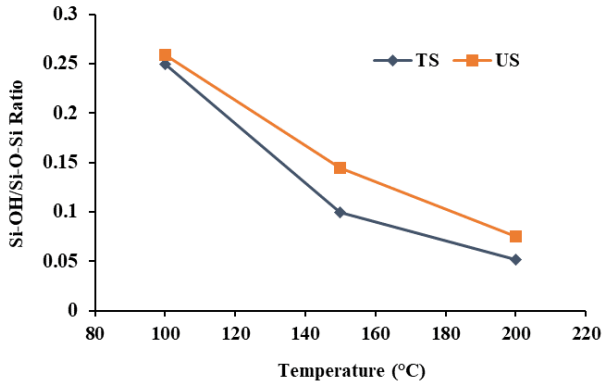


**Figure 6.** The relationship between Si-OH/Si-O-Si ratio with and without ultrasound treatment

The hydrophobic properties of silica-rich sodalites have been shown in Figure 6. A decrease in the ratio of Si-OH/Si-O-Si indicates a decrease in hydrophilic properties or an increase in hydrophobic properties. The changes in silica-rich sodalite's hydrophilic/hydrophobic properties can be seen in the ratio of Si-OH/Si-O-Si. Increasing temperature from 100 to 150°C caused a decrease in the ratio of Si-OH/Si-O-Si by 14.98% without ultrasound treatment and 11.47% with ultrasound. Meanwhile, with the increase in temperature from 150 to 200°C, the ratio decreased by 4.78% without ultrasound and 6.98% with ultrasound.

Meanwhile, ultrasound treatment only reduced the Si-OH/Si-O-Si ratio at the same temperature by 1–4.45%. Thus, increasing the temperature reduces the Si-OH/Si-O-Si ratio effectively. As specified by Yin *et al.* [43], a high hydrothermal treatment temperature can obtain crystallinity and hydrophobic properties.

The more Si-OH groups formed, the more amorphous the phase becomes, causing it to be more soluble in water. In contrast, it can be ascertained that the increasing number of hydrophobic Si-O-Si groups [44] will lead to the formation of more crystalline phases, resulting in the formation of a more structured framework [7]. In conclusion, zeolites can generally be synthesized without or with ultrasound-forming crystals.

### 3.3. Nitrogen Adsorption of Silica-rich Sodalite Zeolite

The gas sorption analyzer (GSA) analysis was only performed on silica-rich sodalite samples with a Si/Al ratio of 30, hydrothermal temperatures of 150 and 200°C because the Si-O-Si framework is more dominant than Si-OH, and prepared with and without ultrasound treatment. The pattern of the adsorption-desorption isotherm is shown in Figure 7.

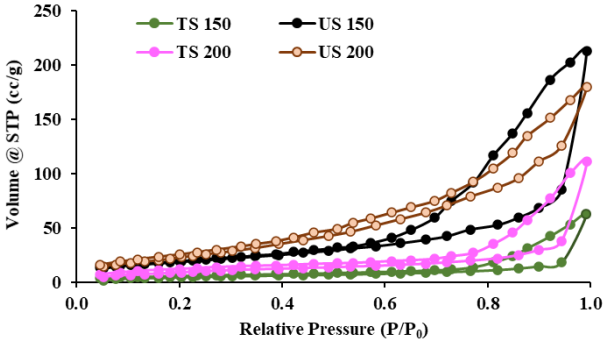


**Figure 7.** The adsorption-desorption isotherm pattern of silica-rich sodalite zeolite with and without ultrasound treatment

Figure 7 shows that silica-rich sodalite zeolite with a Si/Al ratio of 30 is a porous material characterized by hysteresis in its adsorption-desorption isotherm pattern. The pattern also provides information that the ability to adsorb nitrogen gas of silica-rich sodalite with ultrasound treatment at hydrothermal temperatures of 150°C (US 150) and 200°C (US 200) is higher than without ultrasound treatment (TS 150 and TS 200). However, the US 200 showed that low relative pressures ($P/P_0 < 0.2$) could absorb more nitrogen gas, while US 150 was lower and increased significantly at $P/P_0 > 0.8$.

**Table 1.** Surface area, pore size, and pore volume silica-rich sodalite with and without ultrasound treatment

| Sample codes | Surface area ($m^2/g$) | Pore size (Å) | Pore volume (cc/g) |
|---|---|---|---|
| TS 150 | 49.821 | 33.474 | 0.092 |
| US 150 | 114.137 | 33.324 | 0.318 |
| TS 200 | 64.319 | 33.704 | 0.164 |
| US 200 | 160.717 | 46.332 | 0.274 |

Table 1 shows that all sodalite with a Si/Al ratio of 30 has the mesoporous group because pore sizes 33.3–46.3 Å, according to IUPAC size 20–500 Å, belong to mesoporous materials. In addition, ultrasound treatment increased the sample's surface area and pore volume but had a more negligible effect on the pore size [45]. In comparison, the hydrothermal temperature of 200°C with ultrasound succeeded in increasing the pore size significantly. Based on the data analysis, the US 150 sample has more pores (more porous), but the size is smaller than US 200, which is predicted to have a pocket-like shape with a small pore mouth.

## 4. Conclusion

Based on the description of the results and discussion, it can be concluded that the Si/Al ratio of 30 had the highest crystallinity, followed by the ratio of 40 and 20. While the ratio of 60, 80, and 90 indicated that the zeolite obtained was amorphous. Ultrasound treatment and increasing hydrothermal temperatures of 100, 150, and 200°C slightly decreased the crystallinity of silica-rich sodalites. Meanwhile, increasing the hydrothermal temperature without ultrasound treatment increased the crystallinity and hydrophobicity of silica-rich sodalite. Increasing the temperature was more effective than pretreatment ultrasound in reducing the Si-OH/Si-O-Si ratio. Increasing the hydrothermal temperature of 150

and 200°C both with and without ultrasound treatment increased the surface area significantly. Sodalite with the Si/Al ratio of 30 treated with ultrasound had surface areas and pore volumes of 114.137 $m^2/g$ and 0.318 cc/g (US 150), 160.717 $m^2/g$ and 0.274 cc/g (US 200), respectively. Thus, the ability to adsorb nitrogen gas becomes higher.

## Acknowledgment

The authors would like to acknowledge the Directorate General of Research and Development gratefully, the Ministry of Research, Technology and Higher Education of Indonesia for the research funding provided in the 2020 fiscal year with the contract number No. 101-27/UN7.6.1/PP/2020, as well as the Department of Chemistry that has provided facilities for this research to be carried.

## References

[1] N. V. Chukanov, S. M. Aksenov, R. K. Rastsvetaeva, Structural chemistry, IR spectroscopy, properties, and genesis of natural and synthetic microporous cancrinite-and sodalite-related materials: a review, *Microporous and Mesoporous Materials*, 323, 111098, (2021), 1-44 https://doi.org/10.1016/j.micromeso.2021.111098

[2] Orevaoghene Eterigho-Ikelegbe, Samson Bada, Michael O. Daramola, Rosemary Falcon, Synthesis of high purity hydroxy sodalite nanoparticles via pore-plugging hydrothermal method for inorganic membrane development: Effect of synthesis variables on crystallinity, crystal size and morphology, *Materials Today: Proceedings*, 38, 2, (2021), 675-681 https://doi.org/10.1016/j.matpr.2020.03.693

[3] C. L. Eden, M. O. Daramola, Evaluation of silica sodalite infused polysulfone mixed matrix membranes during $H_2/CO_2$ separation, *Materials Today: Proceedings*, 38, 2, (2021), 522-527 https://doi.org/10.1016/j.matpr.2020.02.393

[4] S. Sriatun, H. Susanto, W. Widayat, A. Darmawan, S. Sriyanti, R. Kurniasari, R. Kurniawati, Synthesis of silica-rich zeolite using quaternary ammonium-based templates, *Journal of Physics: Conference Series*, 2020 https://doi.org/10.1088/1742-6596/1524/1/012087

[5] Maria Rubtsova, Ekaterina Smirnova, Sevastyan Boev, Michail Kotelev, Kirill Cherednichenko, Vladimir Vinokurov, Yuri Lvov, Aleksandr Glotov, Nanoarchitectural approach for synthesis of highly crystalline zeolites with a low Si/Al ratio from natural clay nanotubes, *Microporous and Mesoporous Materials*, 330, 111622, (2022), 1-9 https://doi.org/10.1016/j.micromeso.2021.111622

[6] Justyna Szerement, Alicja Szatanik-Kloc, Renata Jarosz, Tomasz Bajda, Monika Mierzwa-Hersztek, Contemporary applications of natural and synthetic zeolites from fly ash in agriculture and environmental protection, *Journal of Cleaner Production*, 311, 127461, (2021), 1-19 https://doi.org/10.1016/j.jclepro.2021.127461

[7] Nan Jiang, Ran Shang, Sebastiaan G. J. Heijman, Luuk C. Rietveld, High-silica zeolites for adsorption of organic micro-pollutants in water treatment: A review, *Water Research*, 144, (2018), 145-161 https://doi.org/10.1016/j.watres.2018.07.017

[8] Norsuhailizah Sazali, Zawati Harun, Tijjani Abdullahi, Faiz Hafeez Azhar, Azlinnorazia Ahmad, Nurul Izwanie Rasli, Norazlianie Sazali, Potential of Transforming Sodalite from Synthesis Kaolin with a Mild Condition of the Hydrothermal Method, *Biointerface Research in Applied Chemistry*, 12, 6, (2022), 7376-7393 https://doi.org/10.33263/BRIAC126.73767393

[9] Meyga Evi Ferama Sari, Suprapto Suprapto, Didik Prasetyoko, Direct synthesis of sodalite from kaolin: the influence of alkalinity, *Indonesian Journal of Chemistry*, 18, 4, (2018), 607-613 https://doi.org/10.22146/ijc.25191

[10] Sriatun, Ranu Luthfi Ananto, Effect of Hydrothermal Time on The Character of High Silica Sodalite, *International Journal of Academic Multidisciplinary Research (IJAMR)*, 5, 10, (2021), 134-137

[11] Reza Khoshbin, Ramin Karimzadeh, Synthesis of mesoporous ZSM-5 from rice husk ash with ultrasound assisted alkali-treatment method used in catalytic cracking of light naphtha, *Advanced Powder Technology*, 28, 8, (2017), 1888-1897 https://doi.org/10.1016/j.apt.2017.04.024

[12] Boitumelo Makgabutlane, Lebea N. Nthunya, Edward N. Nxumalo, Nicholas M. Musyoka, Sabelo D. Mhlanga, Microwave irradiation-assisted synthesis of zeolites from coal fly ash: An optimization study for a sustainable and efficient production process, *ACS Omega*, 5, 39, (2020), 25000-25008 https://doi.org/10.1021/acsomega.0c00931

[13] Danutė Vaičiukynienė, Leonas Jakevičius, Aras Kantautas, Vitoldas Vaitkevičius, Vilimantas Vaičiukynas, The effect of ultrasound on Na-A zeolite synthesis based on sodium aluminosilicate gels and solid materials, *Revista Romana de Materiale*, 50, 4, (2020), 471-477

[14] Natalya E. Gordina, Valery Yu. Prokof'ev, Yuliya N. Kul'pina, Nina V. Petuhova, Sevil I. Gazahova, Olga E. Hmylova, Effect of ultrasound on the synthesis of low-modulus zeolites from a metakaolin, *Ultrasonics Sonochemistry*, 33, (2016), 210-219 https://doi.org/10.1016/j.ultsonch.2016.05.008

[15] Valery Yu Prokof'ev, Natalya E. Gordina, Ekaterina M. Konstantinova, Viktoriya V. Voynova, Tatyana N. Borisova, Thermal treatment of a mixture for the NaP zeolite synthesis based on sodium metasilicate and alumina: Effect of ultrasound, *Materials Chemistry and Physics*, 213, (2018), 76-82 https://doi.org/10.1016/j.matchemphys.2018.03.090

[16] Xiaojun Zeng, Xudong Hu, Hanbin Song, Guohua Xia, Zong-Yang Shen, Ronghai Yu, Martin Moskovits, Microwave synthesis of zeolites and their related applications, *Microporous and Mesoporous Materials*, 323, 111262, (2021), 1-18 https://doi.org/10.1016/j.micromeso.2021.111262

[17] S. Sina Hosseini Boosari, Sonia Eskandari, Abolfazl Shakouri, Mahdi Fathizadeh, Effect of heating period and temperature on the synthesis of nano-beta zeolite assisted by microwaves, *Journal Membrane Science & Technology*, 8, 1, (2018), 1000180 http://dx.doi.org/10.4172/2155-9589.1000180

[18] Geovana Stafin, Edson Cezar Grzebielucka, Sandra Regina Masetto Antunes, Christiane Philippini Ferreira Borges, André Vitor Chaves de Andrade, Suellen Aparecida Alves, Éder Carlos Ferreira de

Souza, Synthesis of zeolites from residual diatomite using a microwave-assisted hydrothermal method, *Waste Management*, 126, (2021), 853-860 https://doi.org/10.1016/j.wasman.2021.04.029

[19] Longjie Cui, Ruyue Han, Lu Yang, Yibo Wu, Rujing Pei, Fuxiang Li, Synthesis and characterization of mesoporous sodalite and investigation of the effects of inorganic salts on its structure and properties, *Microporous and Mesoporous Materials*, 306, 110385, (2020), 1-9 https://doi.org/10.1016/j.micromeso.2020.110385

[20] Sriatun Sriatun, Heru Susanto, Widayat Widayat, Adi Darmawan, Hydrocracking of Coconut Oil on the NiO/Silica-Rich Zeolite Synthesized Using a Quaternary Ammonium Surfactant, *Indonesian Journal of Chemistry*, 21, 2, (2021), 361-375 https://doi.org/10.22146/ijc.55522

[21] Bimo Tunggal Dipowardani, Sriatun Sriatun, Taslimah Taslimah, Sintesis silika kristalin menggunakan surfaktan cetiltrimetilamonium bromida (CTAB) dan trimetilamonium klorida (TMACl) sebagai pencetak pori, *Jurnal Kimia Sains dan Aplikasi*, 11, 1, (2008), 20-28 https://doi.org/10.14710/jksa.11.1.20-28

[22] Yanyan Mu, Yu Zhang, Jiangyang Fan, Cuili Guo, Effect of ultrasound pretreatment on the hydrothermal synthesis of SSZ-13 zeolite, *Ultrasonics Sonochemistry*, 38, (2017), 430-436 https://doi.org/10.1016/j.ultsonch.2017.03.043

[23] Ruben M. Dewes, Heidy Ramirez Mendoza, Mafalda Valdez Lancinha Pereira, Cécile Lutz, Tom Van Gerven, Experimental and Numerical Investigation of the Effect of Ultrasound on the Growth Kinetics of Zeolite A, *Ultrasonics Sonochemistry*, 82, 105909, (2022), 1-7 https://doi.org/10.1016/j.ultsonch.2022.105909

[24] M. Mahima Kumar, Hrudananda Jena, Direct single-step synthesis of phase pure zeolite Na–P1, hydroxy sodalite and analcime from coal fly ash and assessment of their $Cs^{+}$ and $Sr^{2+}$ removal efficiencies, *Microporous and Mesoporous Materials*, 333, 111738, (2022), 1-12 https://doi.org/10.1016/j.micromeso.2022.111738

[25] Jie Luo, Haijun Zhang, Jian Yang, Hydrothermal synthesis of sodalite on alkali-activated coal fly ash for removal of lead ions, *Procedia Environmental Sciences*, 31, (2016), 605-614 https://doi.org/10.1016/j.proenv.2016.02.105

[26] Jintang Li, Xue Zeng, Xiaobing Yang, Chaonan Wang, Xuetao Luo, Synthesis of pure sodalite with wool ball morphology from alkali fusion kaolin, *Materials Letters*, 161, (2015), 157-159 https://doi.org/10.1016/j.matlet.2015.08.058

[27] Jamshid Behin, Hossein Kazemian, Sohrab Rohani, Sonochemical synthesis of zeolite NaP from clinoptilolite, *Ultrasonics Sonochemistry*, 28, (2016), 400-408 https://doi.org/10.1016/j.ultsonch.2015.08.021

[28] Ozgul Dere Ozdemir, Sabriye Piskin, A novel synthesis method of zeolite X from coal fly ash: alkaline fusion followed by ultrasonic-assisted synthesis method, *Waste and Biomass Valorization*, 10, 1, (2019), 143-154 https://doi.org/10.1007/s12649-017-0050-7

[29] Rui Li, Aseem Chawla, Noemi Linares, James G. Sutjianto, Karena W. Chapman, Javier García Martínez, Jeffrey D. Rimer, Corrections to "Diverse Physical States of Amorphous Precursors in Zeolite Sol Gel Syntheses", *Industrial & Engineering Chemistry Research*, 57, 32, (2018), 11258-11258 https://doi.org/10.1021/acs.iecr.8b03506

[30] Julien Devos, Meera A. Shah, Michiel Dusselier, On the key role of aluminium and other heteroatoms during interzeolite conversion synthesis, *RSC Advances*, 11, 42, (2021), 26188-26210 https://doi.org/10.1039/D1RA02887A

[31] Sriatun Sriatun, Taslimah Taslimah, Linda Suyati, Synthesis of Zeolite from Sugarcane Bagasse Ash Using Cetyltrimethylammonium Bromide as Structure Directing Agent, *Indonesian Journal of Chemistry*, 18, 1, (2018), 159-165 https://doi.org/10.22146/ijc.22197

[32] Sriatun Sriatun, Adi Darmawan, Sriyanti Sriyanti, Synthesis and Characterization of Zeolite/Magnetitte Composite from Iron Sand of Marina Beach, *Advanced Science Letters*, 23, 7, (2017), 6524-6526 https://doi.org/10.1166/asl.2017.9672

[33] S. M. Pourali, A. Samadi-Maybodi, Role of gel aging in template-free synthesis of micro and nano-crystalline sodalites, *Chemistry of Solid Materials*, 2, 1, (2014), 21-31

[34] P. Vongvoradit, P. Worathanakul, Fast crystallization of SUZ-4 zeolite with hydrothermal synthesis: Part I temperature and time effect, *Procedia Engineering*, 32, (2012), 198-204 https://doi.org/10.1016/j.proeng.2012.01.1257

[35] Maarten Houlleberghs, Eric Breynaert, Karel Asselman, Ewoud Vaneeckhaute, Sambhu Radhakrishnan, Michael W. Anderson, Francis Taulelle, Mohamed Haouas, Johan A. Martens, Christine E. A. Kirschhock, Evolution of the crystal growth mechanism of zeolite W (MER) with temperature, *Microporous and Mesoporous Materials*, 274, (2019), 379-384 https://doi.org/10.1016/j.micromeso.2018.09.012

[36] Hai-Chen Wang, Silvana Botti, Miguel A. L. Marques, Predicting stable crystalline compounds using chemical similarity, *npj Computational Materials*, 7, 1, (2021), 1-9 https://doi.org/10.1038/s41524-020-00481-6

[37] Tahani Aldahri, Jamshid Behin, Hossein Kazemian, Sohrab Rohani, Synthesis of zeolite Na-P from coal fly ash by thermo-sonochemical treatment, *Fuel*, 182, (2016), 494-501 https://doi.org/10.1016/j.fuel.2016.06.019

[38] Tiffany Yit Siew Ng, Thiam Leng Chew, Yin Fong Yeong, Synthesis of small pore zeolite via ultrasonic-assisted hydrothermal synthesis, *Materials Today: Proceedings*, 16, (2019), 1935-1941 https://doi.org/10.1016/j.matpr.2019.06.071

[39] Pameli Pal, Jugal K. Das, Nandini Das, Sibdas Bandyopadhyay, Synthesis of NaP zeolite at room temperature and short crystallization time by sonochemical method, *Ultrasonics Sonochemistry*, 20, 1, (2013), 314-321 https://doi.org/10.1016/j.ultsonch.2012.07.012

[40] Dipak B. Shukla, Vyomesh P. Pandya, Estimation of crystalline phase in ZSM - 5 zeolites by infrared spectroscopy, *Journal of Chemical Technology &*

*Biotechnology*, 44, 2, (1989), 147-154
https://doi.org/10.1002/jctb.280440206

[41] Eugenii A. Paukshtis, Mariya A. Yaranova, Irina S. Batueva, Bair S. Bal'zhinimaev, A FTIR study of silanol nests over mesoporous silicate materials, *Microporous and Mesoporous Materials*, 288, 109582, (2019), 1-5
https://doi.org/10.1016/j.micromeso.2019.109582

[42] V. V. Potapov, L. T. Zhuravlev, Temperature dependence of the concentration of silanol groups in silica precipitated from a hydrothermal solution, *Glass Physics and Chemistry*, 31, 5, (2005), 661-670
https://doi.org/10.1007/s10720-005-0111-z

[43] Tao Yin, Xuan Meng, Linpeng Jin, Chao Yang, Naiwang Liu, Li Shi, Prepared hydrophobic Y zeolite for adsorbing toluene in humid environment, *Microporous and Mesoporous Materials*, 305, 110327, (2020), 1-11
https://doi.org/10.1016/j.micromeso.2020.110327

[44] Satish A. Mahadik, D. B. Mahadik, V. G. Parale, P. B. Wagh, Satish Gupta, A. Venkateswara Rao, Recoverable and thermally stable superhydrophobic silica coating, *Journal of Sol-Gel Science and Technology*, 62, 3, (2012), 490-494
https://doi.org/10.1007/s10971-012-2753-3

[45] Reza Khoshbin, Ramin Karimzadeh, The beneficial use of ultrasound in free template synthesis of nanostructured ZSM-5 zeolite from rice husk ash used in catalytic cracking of light naphtha: effect of irradiation power, *Advanced Powder Technology*, 28, 3, (2017), 973-982
https://doi.org/10.1016/j.apt.2017.01.001